Single-frequency and tunable operation of a continuous intracavity-frequency-doubled singly resonant optical parametric oscillator

Thu-Hien My, Cyril Drag, and Fabien Bretenaker*

Laboratoire Aimé Cotton, CNRS-Université Paris Sud 11, 91405 Orsay Cedex, France
**Corresponding author: Fabien.Bretenaker@lac.u-psud.fr*

Received February 6, 2008; revised May 19, 2008; accepted May 20, 2008;
posted May 27, 2008 (Doc. ID 92498); published June 24, 2008

A widely tunable continuous intracavity-frequency-doubled singly resonant optical parametric oscillator based on MgO-doped periodically poled stoichiometric lithium tantalate crystal is described. The idler radiation resonating in the cavity is frequency doubled by an intracavity BBO crystal. Pumped in the green, this system can provide up to 485 mW of single-frequency orange radiation. The system is continuously temperature tunable between 1170 and 1355 nm for the idler, 876 and 975 nm for the signal, and between 585 and 678 nm for the doubled idler. The free-running power and frequency stability of the system have been observed to be better than those for a single-mode dye laser. © 2008 Optical Society of America

OCIS codes: 190.4970, 190.2620.

Tunable and ultranarrow linewidth visible sources are mandatory instruments for high-resolution spectroscopy [1] or quantum information processing applications of rare-earth ions embedded in solid-state matrices [2] or color centers in diamond [3]. To our knowledge, until now, dye lasers, which are rather cumbersome and difficult to stabilize, have been the only available sources to fill this need. Besides, no broadly tunable frequency-doubled diode-pumped solid-state lasers (for an example, see [4]) are readily available in the red-orange part of the spectrum. Consequently, the development of an all-solid-state tunable cw source in the visible with a low-frequency noise is a major challenge in this field. For example, we focus here on the wavelength of 606 nm, which corresponds to the transition used to coherently control Pr^{3+} ions.

Optical parametric oscillators (OPOs) are an especially promising approach toward this goal. Indeed, in recent years, the increased availability of novel nonlinear materials and high-power solid-state single-frequency pump sources has led to great advances in the development of cw singly resonant OPOs (SROPOs). In a previous work, we successfully used the recently developed periodically poled near stoichiometric $\mathrm{LiTaO_3}$ (PPSLT) to build a cw SROPO emitting 100 mW in the red and pumped by a commercial green laser [5]. However, the output power of this system was limited by its high threshold and by the onset of thermal effects in the nonlinear crystal owing to the large intracavity power at a visible wavelength. Another way to reach visible wavelengths, which has been successfully applied to perform spectroscopy of ions in a solid with an OPO, consists of building an OPO emitting in the near IR and frequency doubling the idler in a second resonant cavity [6,7]. However, this complicates the system and reduces its overall efficiency. Another possible track consists of doubling or upconverting the IR light resonating inside the OPO cavity. This is potentially more efficient because of the high intensity of the resonating beam [8–13]. This has been experimentally realized in different pulsed regimes [8,14,15]. In the cw regime, Bosenberg *et al.* [16] reported a 629 nm solid-state source pumped by cw Nd:YAG and based on PPLN crystal. In this device, the same crystal is designed to provide the OPO gain and to sum the signal and the remaining pump. This source is quite efficient, but its thermal tunability range is not very broad because the two sections of the nonlinear crystal are at the same temperature. Moreover, in this architecture, one can expect the jitter of the pump source to be completely transferred to the visible radiation. In [5], the choice of a SROPO pumped at 532 nm and resonating on the red signal wave failed to generate more than 100 mW of red output because of thermal effects owing to the nonnegligible residual absorption of the PPSLT in the visible. In the present work, we adopt a smarter strategy that avoids thermal lensing effects by resonating the IR idler wave and performing its intracavity second-harmonic generation (SHG) to achieve efficient red-orange synthesis. This architecture takes advantage of the high near-IR power that can be obtained from SROPOs based on PPSLT [17,18].

Our experimental setup is schematized in Fig. 1. The OPO is pumped at 532 nm by a cw Verdi laser. The nonlinear crystal is a 30-mm-long 5%

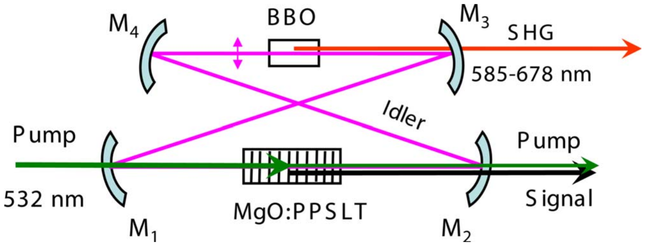

Fig. 1. (Color online) Schematic of the green-pumped intracavity-doubled SROPO (SHG-SROPO). Only the idler (wavelength between 1175 and 1355 nm) resonates in the ring cavity. MgO:PPSLT, parametric gain crystal; BBO, frequency-doubling crystal; M_1–M_4, mirrors.

0146-9592/08/131455-3/$15.00

MgO-doped PPSLT crystal ($d_{\mathrm{eff}} \simeq 11$ pm/V) manufactured and coated by HC Photonics. This crystal contains a single grating with a period of 7.97 μm. It is designed to lead to quasi-phase-matching conditions for an idler wavelength in the 1200–1400 nm range, as already shown in [17,18]. It is antireflection coated for the pump, signal, and idler wavelengths. The crystal temperature can be tuned between 30 and 230 °C.

The 707-mm-long OPO ring cavity is mounted on an Invar base plate and contained in a metal box. It consists of four identical mirrors with a 150 mm radius of curvature. They are designed to exhibit a reflectivity larger than 99.8% between 1.2 μm and 1.4 μm, and a transmission larger than 95% at 532 nm and between 850 and 950 nm to ensure SROPO operation. Then, only the idler is resonant inside the cavity. The SHG crystal is a 10-mm-long beta barium borate (BBO) crystal manufactured and coated by Castech. It is cut at $\theta = 21.1°$ and $\phi = 0°$ to obtain type I phase matching around 1212 nm. Its length is limited to 10 mm to reduce the effect of the walk-off (52 mrad in this case). It is antireflection coated for the idler and red-orange wavelength ranges. The pump beam is focused to a 53 μm waist inside the PPSLT crystal.

Figure 2 shows the SROPO-SHG tuning range as a function of the crystal temperature. The wavelengths are measured with a lambdameter with a 0.02 pm resolution (HighFinesse Angström WSU). By varying the PPSLT crystal temperature from 80 °C to 200 °C, the signal (idler) wavelength can be tuned anywhere between 975 and 876 nm (1170 and 1355 nm). By progressively adjusting the orientation of the BBO crystal with a 2° total excursion, the SHG wavelength can thus be tuned between 585 and 678 nm (the spectral acceptance of the BBO crystal is measured to be equal to 16 nm). The signal power is measured at the output of mirror M_2 (see Fig. 1). The red-orange powers reported in Fig. 2 correspond to the power at the output of the BBO crystal impinging on mirror M_3. Since this mirror has not yet been optimized for transmission of red-orange light, typically only one half (depending on the wavelength) of this power is available at the output of the cavity. Once we have a new mirror M_3 with a maximum transmission in the orange, we can see that a 300 mW output power will be available at 606 nm for a pump power of 6.5 W. In the same time, roughly 2.5 W of signal power is produced in the 876 to 975 nm wavelength range. The bell-like shape of the curves of Fig. 2 is due to the fact that the BBO coatings introduce extra losses on the red side of the curve, and the mirrors exhibit an increase in transmission when the wavelength is shorter than 1200 nm. A flatter tuning profile could be obtained by optimizing the coatings.

With a crystal temperature of 103 °C, we obtain an SHG wavelength of 606.5 nm, for which all the coatings have been optimized. The corresponding evolutions of the SHG and signal (at 948 nm) output powers versus pump power are shown in Fig. 3. The threshold is found to be equal to 4.5 W (4 W without the BBO crystal). From the measured values of the idler output power and the transmission of the mirrors for this wavelength (1213 nm), we deduce the idler intracavity power. It varies from 60 to 180 W when the pump power varies between 4.8 and 7.6 W. Consequently, the SHG efficiency is below or equal to 0.3%. Thus the SHG process can be considered as a small extra loss for the idler and is too weak to modify the OPO stability [13]. In Fig. 3, we find the evolution of the SHG power versus incident pump power to be almost linear, and we checked that it evolves quadratically with the intracavity idler power. This is consistent with the predictions of [9,16]. A maximum SHG output power of 170 mW (485 mW at the BBO output), corresponding to 3 W of signal radiation, for a pump power of 7.6 W, has been obtained. This cw orange output power is large enough for the applications mentioned in the introduction. For pump powers larger than 6 W, we measured pump depletions exceeding 80%.

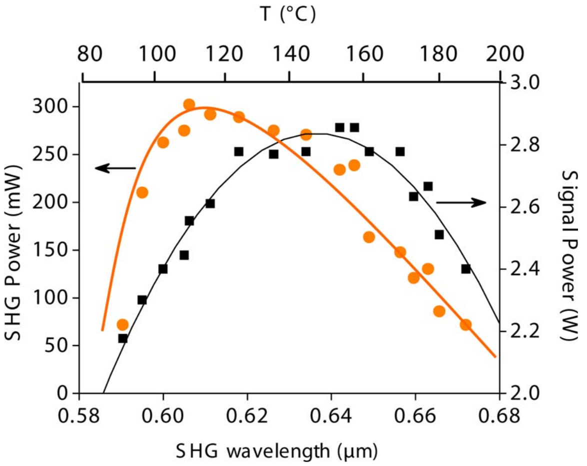

Fig. 2. (Color online) Signal output power (squares) and SHG power at the output of the BBO crystal (circles) versus SHG wavelength and PPSLT crystal temperature for an incident pump power fixed at 6.5 W. The lines are here to guide the eye.

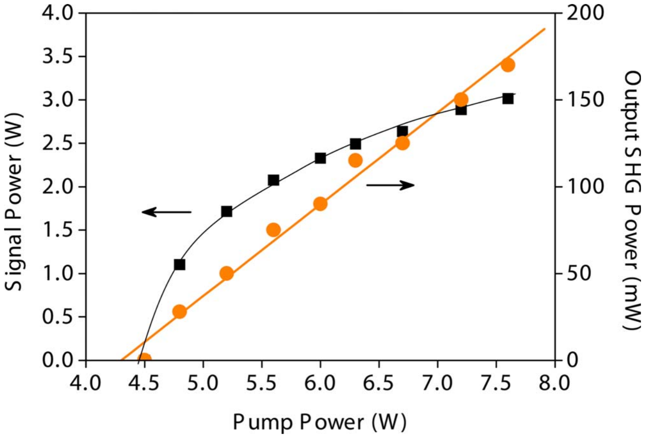

Fig. 3. (Color online) SHG power (circles) mesaured at the output of mirror M_3 and signal power (squares) measured at the output of mirror M_2 versus pump power for a crystal operating at 103 °C. At this wavelength (605.5 nm), the transmission of mirror M_3 is only 35%.

If we want to use the generated orange radiation for high-resolution spectroscopy applications, we need it to be stable and single frequency. We thus analyze the SHG output beam with a scanning confocal Fabry–Perot interferometer (free spectral range, 1 GHz; finesse, 350). The inset of Fig. 4(a) confirms the single-frequency operation of our system. Moreover, Fig. 4(a) shows that the power exhibits an rms stability better than 1.2% over 100 s. These results have been obtained in free-running operation, without any active stabilization, and illustrate the fact that the SHG-SROPO exhibits no mode hop during several minutes, typically. In the same conditions, we have compared the frequency fluctuations of our SHG-SROPO with those of a commercial single-mode dye laser (Spectra-Physics model 380 pumped by a Millenia solid-state laser). The measurements are made during 12 min with the same lambdameter as above and are reproduced in Fig. 4(b). They show that the rms variations of the SHG-SROPO frequency are equal to 9 MHz, much smaller than the 40 MHz value obtained with the dye laser. Moreover, this figure shows that the bandwidth of the frequency fluctuations of the SHG-SROPO seems to be much narrower than the dye laser's one. This indicates that servo-locking the OPO frequency should be feasible.

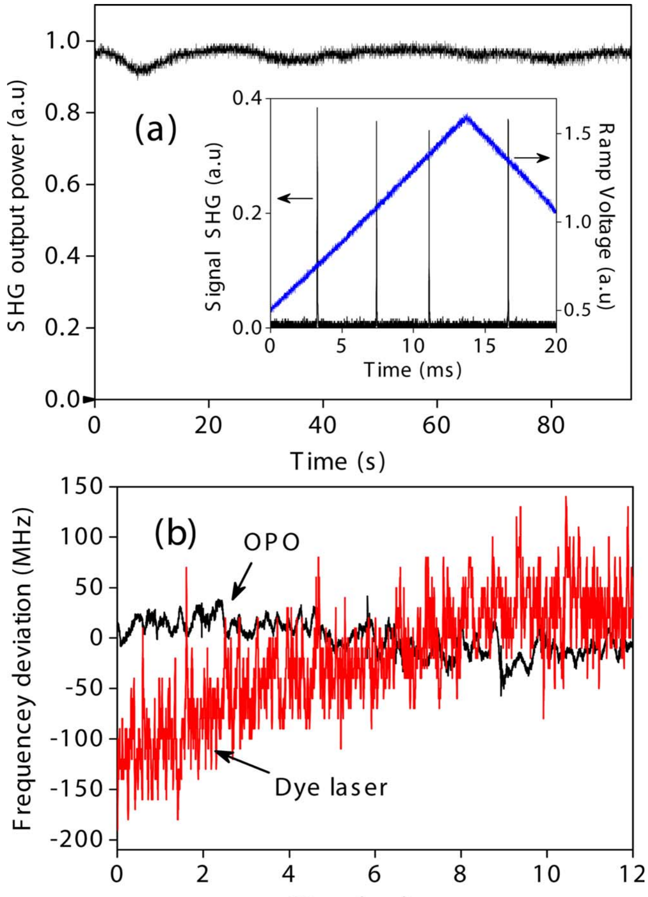

Fig. 4. (Color online) Free-running OPO stability measurements for a 6.5 W pump power and a SHG wavelength equal to 606 nm. (a) SHG power versus time. The rms noise is equal to 1.2%. The maximum relative level 1.0 corresponds to 100 mW red output power. Inset, SHG intensity analyzed by a scanning confocal Fabry–Perot cavity versus time (left scale) and voltage applied to the piezoelectric transducer of the cavity (right scale). (b) Free-running frequency deviations of the SHG-SROPO and of a commercial dye laser versus time. Sampling frequency, 10 Hz.

In conclusion, we have built a green-pumped cw intracavity-frequency-doubled singly resonant optical parametric oscillator, based on PPSLT and BBO crystals. This system operates in single frequency at the three wavelengths and is tunable over more than 90 nm in the visible, without any optimization of the coatings for tunability. Maximum powers of 485 mW in the orange and 3 W at 948 nm can be obtained with a pump power of 7.6 W. The long-term stability of the output beam confirms that its frequency is naturally more stable than that of a commercial dye laser. This result is very promising for future stabilizations of the SHG frequency of our system. In future work, we plan to (i) optimize the cavity in order to obtain more power, (ii) stabilize the SHG frequency by using the Pound–Drever–Hall technique, and (iii) study the fine tuning capabilities of this OPO by introducing a specially optimized etalon in the cavity.

References

1. R. Klieber and D. Suter, Phys. Rev. B **73**, 094408 (2006).
2. J. J. Longdell, M. J. Sellars, and N. B. Manson, Phys. Rev. Lett. **93**, 130503 (2004).
3. P. R. Hemmer, A. V. Turukhin, M. S. Shahriar, and J. A. Musser, Opt. Lett. **26**, 361 (2001).
4. R. Sarrouf, V. Sousa, T. Badr, G. Xu, and J.-J. Zondy, Opt. Lett. **32**, 2732 (2007).
5. J.-M. Melkonian, T.-H. My, F. Bretenaker, and C. Drag, Opt. Lett. **32**, 518 (2007).
6. T. Petelski, R. S. Conroy, K. Bencheikh, J. Mlynek, and S. Schiller, Opt. Lett. **26**, 1013 (2001).
7. U. Strössner, J.-P. Meyn, R. Wallenstein, P. Urenski, A. Arie, G. Rosenman, J. Mlynek, S. Schiller, and A. Peters, J. Opt. Soc. Am. B **19**, 1419 (2002).
8. A. J. Campillo and C. L. Tang, Appl. Phys. Lett. **19**, 36 (1971).
9. T. G. Giallorenzi and M. H. Reilly, IEEE J. Quantum Electron. **8**, 302 (1972).
10. P. P. Bey and C. L. Tang, IEEE J. Quantum Electron. **8**, 361 (1972).
11. G. T. Moore and K. Koch, IEEE J. Quantum Electron. **29**, 961 (1993).
12. G. T. Moore and K. Koch, IEEE J. Quantum Electron. **29**, 2334 (1993).
13. G. T. Moore, K. Koch, and E. C. Cheung, Opt. Commun. **113**, 463 (1995).
14. R. J. Ellingson and C. L. Tang, Opt. Lett. **18**, 438 (1993).
15. E. C. Cheung, K. Koch, and G. T. Moore, Opt. Lett. **19**, 1967 (1994).
16. W. R. Bosenberg, J. I. Alexander, L. E. Myers, and R. W. Wallace, Opt. Lett. **23**, 207 (1998).
17. G. K. Samanta, G. R. Fayaz, Z. Sun, and M. Ebrahim-Zadeh, Opt. Lett. **32**, 400 (2007).
18. G. K. Samanta, G. R. Fayaz, and M. Ebrahim-Zadeh, Opt. Lett. **32**, 2623 (2007).